Human Molecular Genetics, 2004, Vol. 13, No. 11 **1159–1170**
DOI: 10.1093/hmg/ddh125
Advance Access published on March 31, 2004

Disruption of the *WFS1* gene in mice causes progressive β-cell loss and impaired stimulus–secretion coupling in insulin secretion

Hisamitsu Ishihara[1], Satoshi Takeda[4], Akira Tamura[1], Rui Takahashi[1], Suguru Yamaguchi[1], Daisuke Takei[1], Takahiro Yamada[1], Hiroshi Inoue[5], Hiroyuki Soga[2], Hideki Katagiri[3], Yukio Tanizawa[6] and Yoshitomo Oka[1,*]

[1]Division of Molecular Metabolism and Diabetes, [2]Division of Immunology and Embryology, and [3]Division of Advanced Therapeutics for Metabolic Diseases, Tohoku University Graduate School of Medicine, Sendai, Japan, [4]Otsuka GEN Research Institute, Otsuka Pharmaceutical Co., Tokushima, Japan, [5]Division of Diabetes and Endocrinology, Department of Medicine, Kawasaki Medical School, Kurashiki, Japan and [6]Division of Molecular Analysis of Human Disorders, Department of Bio-Signal Analysis, Yamaguchi University Graduate School of Medicine, Ube, Japan

Received February 8, 2004; Revised and Accepted March 26, 2004

Wolfram syndrome, an autosomal recessive disorder characterized by juvenile-onset diabetes mellitus and optic atrophy, is caused by mutations in the *WFS1* gene. In order to gain insight into the pathophysiology of this disease, we disrupted the *wfs1* gene in mice. The mutant mice developed glucose intolerance or overt diabetes due to insufficient insulin secretion *in vivo*. Islets isolated from mutant mice exhibited a decrease in insulin secretion in response to glucose. The defective insulin secretion was accompanied by reduced cellular calcium responses to the secretagogue. Immunohistochemical analyses with morphometry and measurement of whole-pancreas insulin content demonstrated progressive β-cell loss in mutant mice, while the α-cell, which barely expresses WFS1 protein, was preserved. Furthermore, isolated islets from mutant mice exhibited increased apoptosis, as assessed by DNA fragment formation, at high concentration of glucose or with exposure to endoplasmic reticulum-stress inducers. These results strongly suggest that WFS1 protein plays an important role in both stimulus–secretion coupling for insulin exocytosis and maintenance of β-cell mass, deterioration of which leads to impaired glucose homeostasis. These WFS1 mutant mice provide a valuable tool for understanding better the pathophysiology of Wolfram syndrome as well as WFS1 function.

INTRODUCTION

Wolfram syndrome (OMIM 222300) is a rare autosomal recessive disorder characterized by juvenile-onset non-autoimmune diabetes mellitus, optic atrophy, sensorineural deafness and diabetes insipidus (1). In addition, psychiatric illnesses such as depression and impulsive behavior are frequently observed in affected individuals (2). The nuclear gene responsible for this syndrome was identified by us (3) and others (4), and designated *WFS1* (3). More than 100 mutations of the *WFS1* gene have been identified to date in Wolfram syndrome patients. Most are inactivating mutations, suggesting loss of function to be responsible for the disease phenotype (5). WFS1 mutations underlie not only autosomal recessive Wolfram syndrome but also autosomal dominant low-frequency sensorineural hearing loss (LFSNHL). Heterozygous, non-inactivating WFS1 mutations were recently found in families with LFSNHL linked to chromosome 4p16 (DFNA6/14/38) (OMIM 600965) (6,7). The observation that the first-degree relatives of Wolfram syndrome patients have increased frequencies of diabetes mellitus and certain psychiatric disorders suggests sequence variants of the *WFS1* gene predispose these individuals to such conditions (2,8). Indeed, several WFS1 sequence variants have been shown to be significantly associated with more common forms of diabetes mellitus (9,10) as well as with suicidal and impulsive behavior (11).

*To whom correspondence should be addressed at: Division of Molecular Metabolism and Diabetes, Tohoku University Graduate School of Medicine, 2-1 Seiryo-machi, Aoba-ku, Sendai 980-8575, Japan. Tel: +81 227177173; Fax: +81 227177179; Email: oka@int3.med.tohoku.ac.jp

The WFS1 protein, also called wolframin (4), consists of 890 amino acids and was predicted to have nine or ten membrane spanning domains (3,4). Proteins with sequence similarity are now found in public databases of other organisms, *Drosophila melanogaster* (CG4917), *Anopheles gambiae* (EBIP3764) and *Fugu rubripes* (SINFRUP82345), but little is known about their functions, suggesting WFS1 protein to belong to a novel family. The WFS1 protein is expressed in various tissues but at higher levels in the brain, heart, lung and pancreas (3,4). We showed the WFS1 protein to be localized predominantly in the endoplasmic reticulum (ER) and suggested a possible role of this protein in membrane trafficking, protein processing and/or regulation of cellular calcium homeostasis (12). A recent study showed this protein to contain nine transmembrane domains and to be embedded in the ER membrane with the amino-terminus in the cytosol and the carboxy-terminus in the ER lumen (13). ER dysfunction is known to cause apoptosis, which underlies a number of genetic disorders (14,15), possibly including a subset of diabetes (15). Since severe atrophic changes have been reported in the brain and in pancreatic islets of subjects with Wolfram syndrome (16,17), it is reasonable to speculate that WFS1 protein plays an essential role in the survival of neuronal cells and islet β-cells.

In this study, to gain insight into the pathophysiology of Wolfram syndrome, we disrupted the *wfs1* gene in mice. The mice developed glucose intolerance or overt diabetes, depending on their genetic background. Our results demonstrate that the impaired glucose homeostasis in these mice results from insufficient insulin secretion due to defects in both stimulus–secretion coupling and maintenance of β-cell mass.

RESULTS

Targeted disruption of the *WFS1* gene

We first studied wfs1 protein expression in the pancreas, as this was essential to understand the diabetic phenotype in mice with a disrupted *wfs1* gene. Mouse pancreas sections were stained using an antibody raised against the 290 amino acid amino-terminus peptide of murine WFS1 (α-mWFS1-N) and those against islet hormones (Fig. 1A–L). Importantly, the WFS1 protein is strongly expressed in β-cells, and the majority of α, δ and F-cells are essentially devoid of wfs1 protein immunoreactivity. Double-staining of dispersed islet cells with these antibodies showed >80% of insulin-positive cells to be stained with anti-WFS1 antibody, while few cells express both WFS1 protein and one of the following: glucagon, somatostatin or pancreatic polypeptide (Fig. 1M–P).

In order to study the pathophysiology of Wolfram syndrome, we sought to inactivate the *wfs1* gene by inserting a neomycin-resistance gene into the second exon of the *wfs1* gene which contains the initial ATG codon (Fig. 2A and B). When analyzed using an antibody against α-mWFS1-N, WFS1 protein bands of 95 kDa were abolished in whole-brain lysates from mutant mice (Fig. 2C). In addition, WFS1 protein staining was detected in neither pancreatic islets (Fig. 2D and E) nor the hippocampus (Fig. 2F and G) in mutant animals. It was subsequently recognized that our disruption strategy resulted in altered splicing transcripts in mutant animals. Reverse transcription–polymerase chain reaction on brain, heart and islet mRNA revealed existence of a *wfs1* mRNA that lacks exon 2 in mutant animals (data not shown). Such an altered mRNA was not detected in wild-type tissues. The mutant transcript could generate amino-terminus-truncated WFS1 protein resulting from initiation of translation from one of the internal methionines. There exist methionine residues at 81, 184, 230 and 299, as well as further downstream, in murine WFS1 protein. We constructed a cDNA encoding WFS1 protein lacking the first 80 amino acids (WFS1-del80) and expressed it in COS7 cells. The WFS1-del80 protein was recognized by the antibody α-mWFS1-N (data not shown), while no bands were detected in brain lysates from mutant animals (Fig. 2C), indicating that WFS1-del80 is not expressed in mutant mice and that mutant proteins, if present, would be WFS1 protein lacking the first 183 amino acids or with larger truncations. We speculate that such truncated WFS1 proteins do not have normal functions since human substitution mutations at alanine 126, alanine 133 or glutamate 169 and a deletion mutation that lacks both lysine 178 and alanine 179 residues cause Wolfram syndrome (5). Therefore, we conclude that WFS1 function is lost, or at least severely impaired, in mice with a disrupted *wfs1* gene.

Mice homozygous for the mutated *wfs1* gene constitute the expected 25% of offspring born to heterozygous mutant parents, and are normal in appearance, growth and fertility. We did not see ataxic posture or gait disturbance. In addition, there were no differences in urine osmolality between wild-type and mutant mice. In the following experiments only male mice were used because an earlier study indicated females to have a milder phenotype. Since juvenile-onset diabetes mellitus is the most prominent feature of Wolfram syndrome, we have focused on this issue herein. Detailed studies on other aspects of this syndrome, including optic atrophy, hearing disorders, diabetes insipidus or psychiatric illness, are currently underway.

Impaired glucose homeostasis in mutant mice

Blood glucose levels in these mice were studied in non-fasted states. Initially, using mice on the [(129Sv × B6) × B6]F2 hybrid background, we found that blood glucose levels of mutant mice started to rise at around 16 weeks of age and >60% of mice (8 out of 13) had overt diabetes by 36 weeks (Fig. 3A). Since the heterogeneous contribution of B6 and 129Sv strains in the mixed background mice could cause a large variance in data, making interpretation difficult, we sought to generate mutant animals on a nearly homogenous genetic background. For this purpose, male mice with a disrupted *wfs1* gene were backcrossed for five successive generations with female mice of the B6 strain, which is frequently used for diabetes and obesity research. On the B6 background, no apparent increase in blood glucose levels was observed even at 36 weeks in mice homozygous for disrupted *wfs1* alleles (Fig. 3B). However, impaired glucose homeostasis was evident in mice on the B6 background when they were subjected to oral glucose tolerance test (Fig. 3C). Blood glucose levels at 15 and 30 min were significantly higher in mutant than in wild-type mice at 17 weeks of

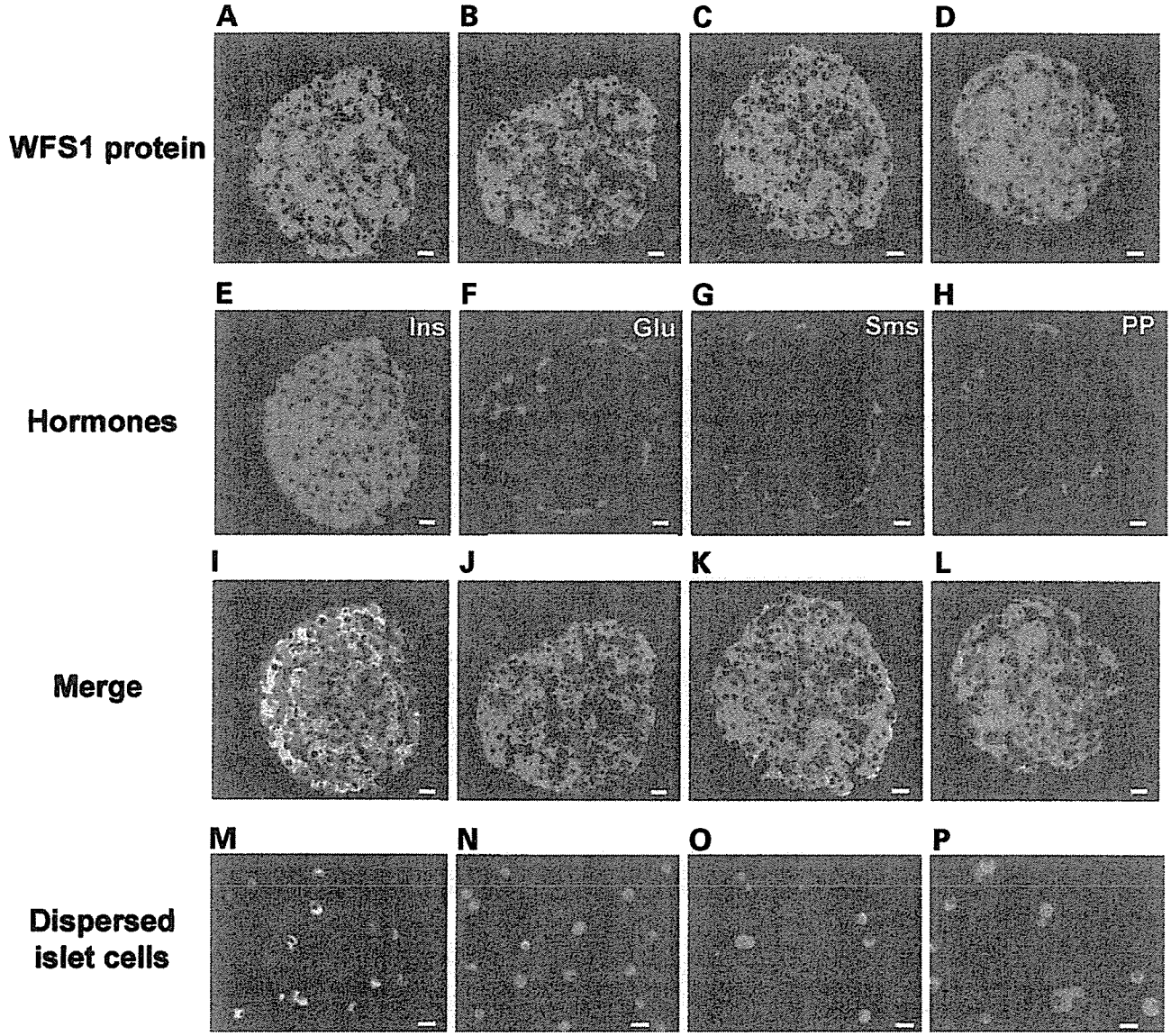

Figure 1. β-Cell specific expression of WFS1 protein in the pancreas. (**A–L**) Paraffin embedded mouse pancreatic sections were immunostained with antibodies against WFS1 protein (green) (A–D) and islet hormones (red): insulin (E), glucagon (F), somatostatin (G), or pancreatic polypeptide (H). A and E are the same section, and the two are merged in I. Similarly, J, K, L are merged versions of B and F, C and G, D and H, respectively. Bars = 10 μm. Ins, insulin; Glu, glucagon; Sms, somatostatin; PP, pancreatic polypeptide. (**M–P**) Dispersed islet cells were stained with anti-WFS1 antibody (green) together with those against islet hormones (red): insulin (M), glucagon (N), somatostatin (O) or pancreatic polypeptide (P). Bars = 10 μm.

age. These data indicated that disruption of the *wfs1* locus induced impaired glucose homeostasis in mice, as is seen in human Wolfram syndrome.

In order to investigate the pathophysiology of impaired glucose homeostasis in mutant mice, plasma immunoreactive insulin (IRI) levels in response to a glucose load were evaluated. Although plasma insulin levels after a 6 h fast were comparable between wild-type and mutant animals at 17 weeks of age (Fig. 3D), hormone responses were markedly blunted in WFS1-deficient mice. We also studied non-fasting plasma insulin levels in these mice. Plasma insulin levels in mutant mice were similar to that in wild-type mice at 24 weeks but had decreased to half the wild-type level at 36 weeks (Fig. 3E). Intraperitoneal insulin injection tests did not show insulin resistance in mutant mice at 14 (data not shown) and 19 weeks (Fig. 3F). In fact, WFS1-deficient mice were somewhat more insulin sensitive. Taken together, these data indicate impaired glucose homeostasis in mice with a disrupted *wfs1* gene to be due to insulin secretory defects rather than insulin resistance.

Impaired stimulus–secretion coupling in β-cells from mutant mice

Since defects in both stimulus–secretion coupling and insulin production could be the cause of insulin secretory defects *in vivo*, insulin secretory responses were studied using isolated islets. When we isolated islets from these mice, we noticed that

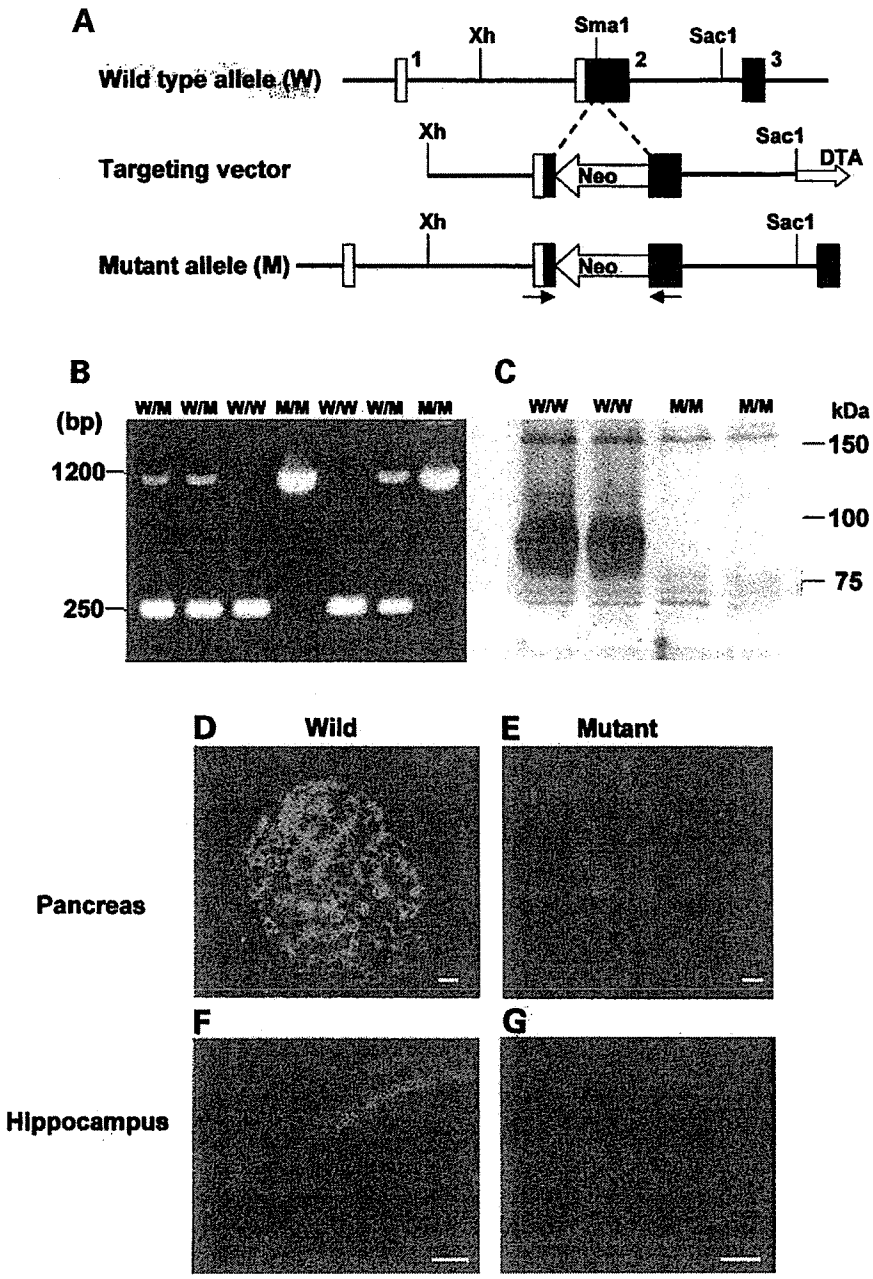

Figure 2. Targeted disruption of the *WFS1* gene. (**A**) Schematic representation of the mouse *wfs1* targeting strategy. Boxes are exons. Neo, neomycin resistance gene; DTA, diphtheria toxin A chain gene. (**B**) PCR genotyping of mutant mice. A 1200 bp longer band is observed in DNA from the disrupted allele. (**C**) Western blot analysis using whole-brain lysates from wild-type and mutant animals probed with anti-WFS1 antibody. (**D–G**) Immunohistochemical analyses using anti-WFS1 antibody in pancreatic (D, E) and hippocampal (F, G) tissues from 14-week-old wild-type and mutant mice. Bars = 10 μm for pancreatic sections and 50 μm for hippocampal sections.

it was possible to obtain only 100 islets or even less from a mutant mouse, while around 200 islets can normally be isolated from a wild-type mouse. Insulin content in the WFS1-deficient islets was slightly (16%) but significantly less than that in islets of wild-type mice [61.8 ± 2.3 ng/islet ($n = 10$ experiments) versus 73.4 ± 3.3 ($n = 10$ experiments), $P = 0.039$, mutant and wild-type islets, respectively]. We used these islets infected with either AdCAGlacZ (as a control) or AdCAGmWFS1 (Fig. 4A), because we also wanted to examine effects of WFS1 re-expression in WFS1-deficient islets and of its overexpression in wild-type islets. Glucose (15 mM)-stimulated insulin secretion, after normalization with insulin content, was reduced by 23% in islets from mutant mice (Fig. 4B). Carbachol (1.0 mM)-stimulated insulin secretion, which is thought to be evoked by Ca^{2+} release from the ER and Ca^{2+} entry through the Ca^{2+} release-activated channel, was also reduced by 26% (Fig. 4C). When WFS1 protein was re-expressed in islets from mutant animals via a recombinant adenovirus,

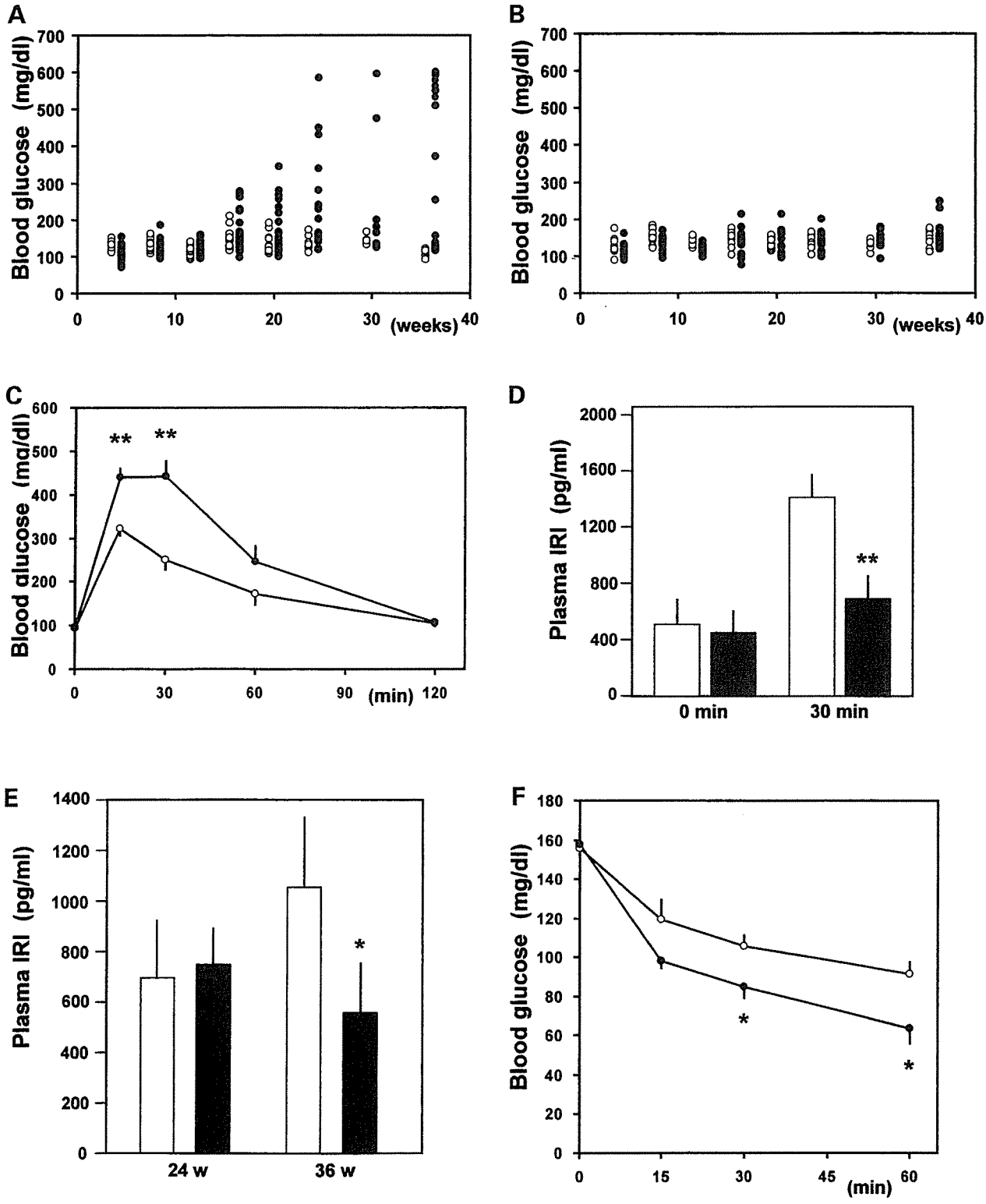

Figure 3. Impaired glucose homeostasis in WFS1-deficient mice. (**A**) Non-fasted blood glucose levels in male mice on the [(129Sv × B6) × B6]F2 hybrid background at indicated ages ($n = 8–13$). (**B**) Non-fasted blood glucose levels in male mice on the B6 background ($n = 9–16$). (**C, D**) Oral glucose (2 mg/g body weight) tolerance test in 17-week-old mice on the B6 background ($n = 6$). Blood glucose levels (C) at indicated points and plasma IRI levels (D) before and 30 min after the glucose load are shown. Glucose tolerance tests were performed on two other occasions using different animals with essentially same results. (**E**) Plasma IRI levels at 24 and 36 weeks of age ($n = 6–8$). (**F**) Insulin (0.75 units/kg body weight) tolerance test at 19 weeks ($n = 5$). Insulin tolerance tests were performed on two other occasions with essentially same results. White circles and bars, wild-type mice; black circles and bars, mutant mice. $^{*}P < 0.05$, $^{**}P < 0.01$.

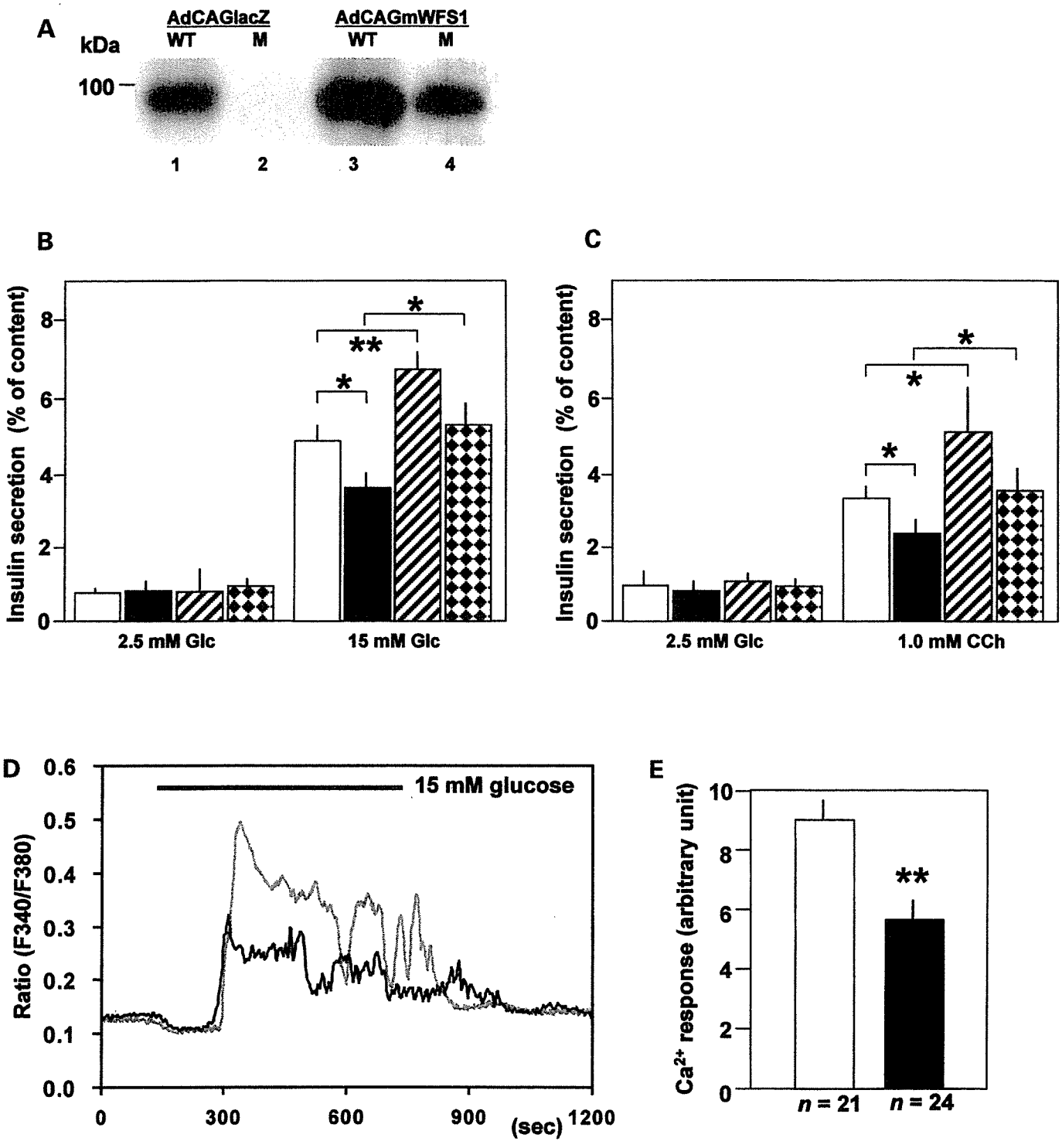

Figure 4. Impaired stimulus–secretion coupling in WFS1-deficient β-cells. (**A**) Islets from wild-type and mutant mice were infected with either AdCAGlacZ or AdCAGmWFS1. After 36 h, islets were subjected to western blot analyses using anti-WFS1 antibody. Lane 1, wild-type islets infected with AdCAGlacZ; lane 2, mutant islets infected with AdCAGlacZ; lane 3, wild-type islets infected with AdCAGmWFS1; lane 4, mutant islets infected with AdCAGmWFS1. Western blot experiments were performed twice with similar results and one of them is shown. (**B, C**) Islets were challenged with 15 mM glucose (B) or 1 mM carbachol in the presence of 2.5 mM glucose (C) for 1 h. Absolute insulin secretion in response to glucose was 3.11 ± 0.34 and 2.03 ± 0.26 ng/islet/h, respectively, for wild-type and mutant islets infected with the control virus (AdCAGlacZ). Data are means ± SEM, $n = 5$ experiments. White bars, wild-type islets infected with AdCA-lacZ; black bars, mutant islets with AdCAGlacZ; hatched bars, wild-type islets with AdCAGmWFS1; dotted bars, mutant islets with AdCAGmWFS1. (**D, E**) Intracellular Ca^{2+} responses to 15 mM glucose in wild-type (gray line and white bar) and WFS1-deficient (black line and black bar) β-cells. Representative traces out of 21 wild-type and 24 WFS1-deficient β-cells from one experiment were shown in D. Areas under the curve during a 5 min period after the onset of Ca^{2+} rises to glucose were summarized in E. Similar significant differences were observed in the other four experiments. $^*P < 0.05$, $^{**}P < 0.01$.

glucose- and carbachol-stimulated insulin secretion was restored (Fig. 4B and C), indicating reduced insulin secretion in islets from mutant mice to be a direct consequence of absence of normal WFS1 function. Interestingly, glucose- and carbachol-stimulated insulin secretion from wild-type islets increased by 41 and 53%, respectively, with overexpression of the WFS1 protein, suggesting involvement of the WFS1 protein in stimulus–secretion coupling for insulin exocytosis (Fig. 4B and C).

To gain insight into the mechanisms of impaired insulin secretion in islets from mutant mice, intracellular calcium dynamics were then studied in single β-cells challenged with glucose. The glucose-stimulated rise in the cytosolic Ca^{2+} response was reduced by 36% in WFS1-deficient β-cells when compared with that in wild-type β-cells (Fig. 4D and E).

Progressive β-cell loss in mutant mice

We then focused on aspects of insulin production, deterioration of which could be a cause of impaired glucose homeostasis in mice with disruption of the *wfs1* gene. There were no differences in pancreatic weight between wild-type and mutant mice (data not shown). Whole-pancreas insulin content was already decreased at 2 weeks, the earliest age studied, and dropped further with age (Fig. 5A). Immunohistochemical studies (Fig. 5B–E) showed the number of insulin-positive cells to be reduced at 36 weeks in the mutant mouse pancreas (Fig. 5E). Morphometric analysis demonstrated a marked reduction in the insulin-positive area per pancreatic area in mutant mice when compared with wild-type mice (Fig. 5H), indicating the decrease in insulin content to be due to loss of islet β-cells. These features were more prominent in the mutant mouse pancreas on the [(129Sv × B6) × B6]F2 background, which was associated with overt diabetes (Fig. 5F and G). In contrast to the β-cell changes, glucagon-positive cells were increased and scattered throughout WFS1-deficient islets (Fig. 5E and G). Indeed, the pancreatic glucagon content in mutant mice at 36 weeks of age on the B6 background was 2.4-fold higher than that in wild-type mice [12.3 ± 1.8 ng/mg ($n = 4$) versus 5.2 ± 0.7 ($n = 4$), $P = 0.0296$].

Increased susceptibility of WFS1-deficient islets to apoptosis

To study whether the observed β-cell loss was due to increased apoptosis, we conducted an extensive search for apoptotic β-cells in pancreatic sections. However, TUNEL or activated-caspase 3-positive cells were sparse within islets in pancreatic sections from both mutant and wild-type animals (data not shown). Therefore, we turned to *in vitro* studies, and examined whether WFS1-deficient islet cells are more susceptible to apoptotic insults. For this purpose, apoptotic DNA fragmentation was studied in isolated islets by the ligation-mediated PCR (LM-PCR) method. When islets were cultured for 3 days in RPMI media with 5 or 25 mM glucose, ladder formation was increased at 25 mM glucose in both wild-type and mutant islets when compared with that at 5 mM glucose, indicating that apoptotic cell death may have been induced by glucose toxicity (Fig. 6A). Importantly, at 25 mM glucose, islets from mutant mice showed more DNA fragment formation than wild-type islets (1.7 ± 0.3-fold, $n = 5$), while no significant differences were observed at 5 mM glucose. Since recent studies have suggested so-called ER-stress to be an important mediator of apoptosis in β-cells (14,15), DNA fragmentation was studied after treatment with two different ER-stress inducers (18), tunicamycin (2 μg/ml) and thapsigargin (2 μM). DNA fragmentation at 5 mM glucose was significantly increased, by 2.2 ± 0.4-fold and 2.4 ± 0.4-fold after tunicamycin (Fig. 6B) and thapsigargin (Fig. 6C) treatments, respectively, in WFS1-deficient islets when compared with wild-type islets. In contrast, there were no differences in DNA fragmentation after combined tumor necrosis factor-α and interferon-γ treatment (Fig. 6D), which triggers apoptosis through a signaling pathway different from that originating in the ER.

DISCUSSION

We generated mice with a disrupted *wfs1* gene. Although the diabetic phenotype was milder than that seen clinically in Wolfram syndrome (1), the progressive β-cell loss and impaired glucose homeostasis observed in these mice are essentially consistent with findings in patients (1,17). Thus, the mutant mice are indeed a model of Wolfram syndrome. The underlying anatomic condition of this syndrome has not been studied in great detail in humans, and the cellular basis for the diabetic phenotype and associated neuro-psychiatric disorders remains obscure. Creation of an animal model that reflects aspects of the disease is thus an important first step in understanding Wolfram syndrome.

The present data demonstrate that the pathophysiological basis of diabetes in Wolfram syndrome is insufficient insulin secretion due to progressive β-cell loss and impaired stimulus–secretion coupling in β-cells. Progressive β-cell loss has been expected from clinical observations of progressive deterioration of insulin-requiring states in affected patients as well as their postmortem findings, i.e. selective β-cell loss with an increase in α-cells and preservation of δ-cells (17). In contrast, impaired stimulus–secretion coupling in the β-cell, a quite unexpected result, was demonstrated for the first time in this study. In addition, we also showed for the first time that WFS1 protein is expressed selectively in β-cells, but very little in α, δ and F-cells, within the endocrine pancreas, suggesting that β-cell loss is a direct consequence of WFS1 deficiency.

The severity of the diabetic phenotype due to *wfs1* gene disruption was dependent on the mouse genetic background: >60% of mice on the [(129Sv × B6) × B6]F2 background developed overt diabetes, while mutant mice on the B6 background had impaired glucose tolerance but not overt diabetes. Modifying effects of genetic background on glucose homeostasis have been reported previously in a number of mutant mice. An earlier pioneering study established that the B6 background confers more diabetes resistance to db/db and ob/ob mice (19). A diabetes-resistant phenotype has also been reported in insulin receptor substrate (IRS)-2 knockout mice on the B6 background (20), while anti-sense glucokinase-mRNA expressing mice (21) and mice double heterozygous for deletion of the insulin receptor and IRS-1 (22), on the same B6 background, were reportedly diabetes prone. Therefore, the

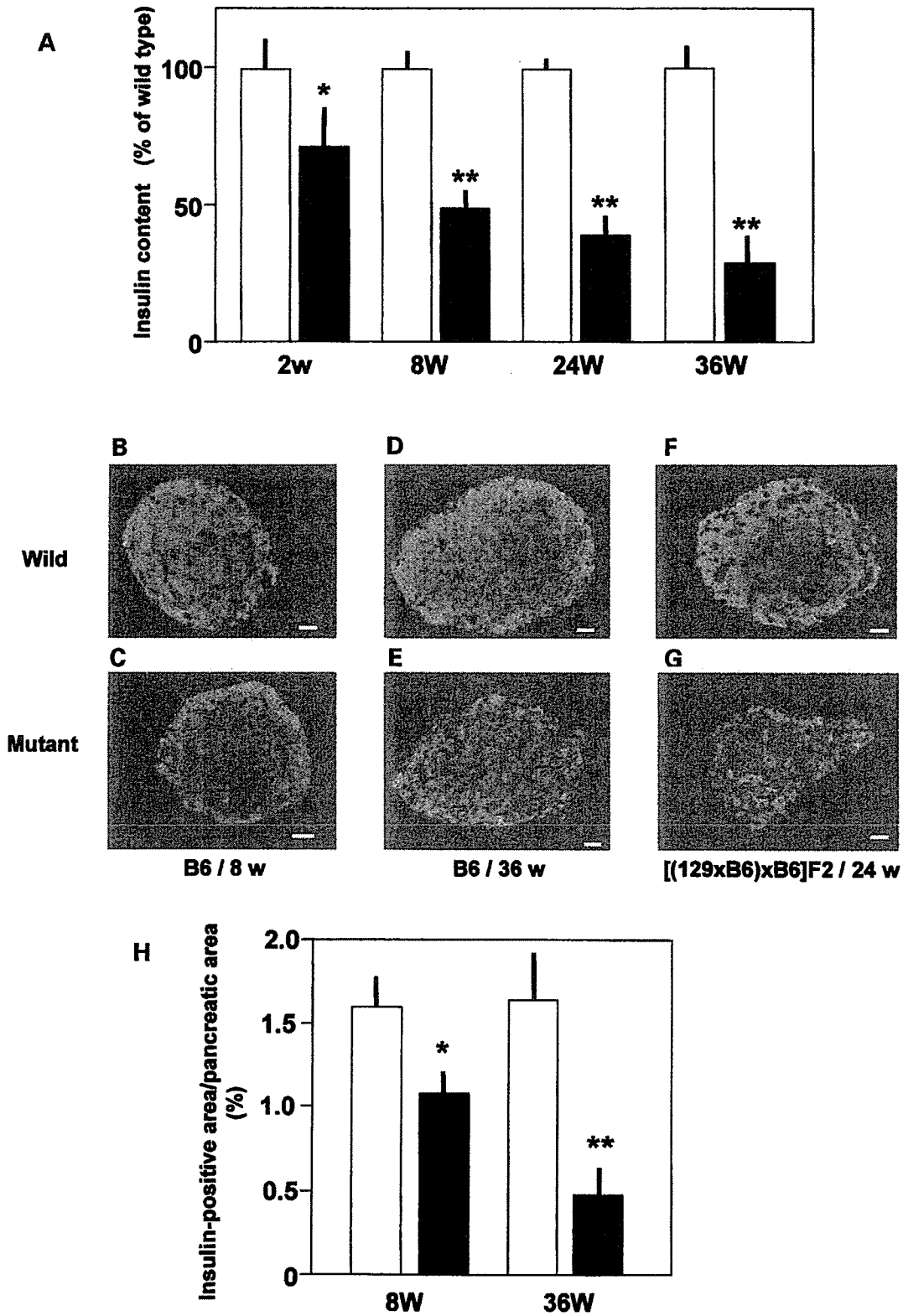

Figure 5. Progressive β-cell loss in mutant mice. (**A**) Insulin content extracted from whole pancreata of wild-type and mutant mice. Data represent percent of insulin content in wild-type littermates. Absolute insulin content in wild-type pancreata were 1367 ± 103 ng/mg pancreas at 2 weeks, 268 ± 18 (8 weeks), 329 ± 25 (24 weeks) and 372 ± 33 (36 weeks), $n = 4–7$. White bars, wild-type pancreata; black bars, WFS1-deficient pancreata. (**B–G**) Insulin (green) and glucagon (red) are stained in pancreatic sections from 8-week-old wild-type (B), mutant (C), 36-week-old wild-type (D) and mutant mice (E) on the B6 background, and 24-week-old wild-type (F) and mutant (G) mice on the [(129Sv × B6) × B6]F2 background. Bars = 10 μm. (**H**) Ratios of total insulin-positive area per whole pancreatic area in pancreas from wild-type and mutant mice on the B6 background. $n = 4$ animals for each group. $^*P < 0.05$, $^{**}P < 0.01$.

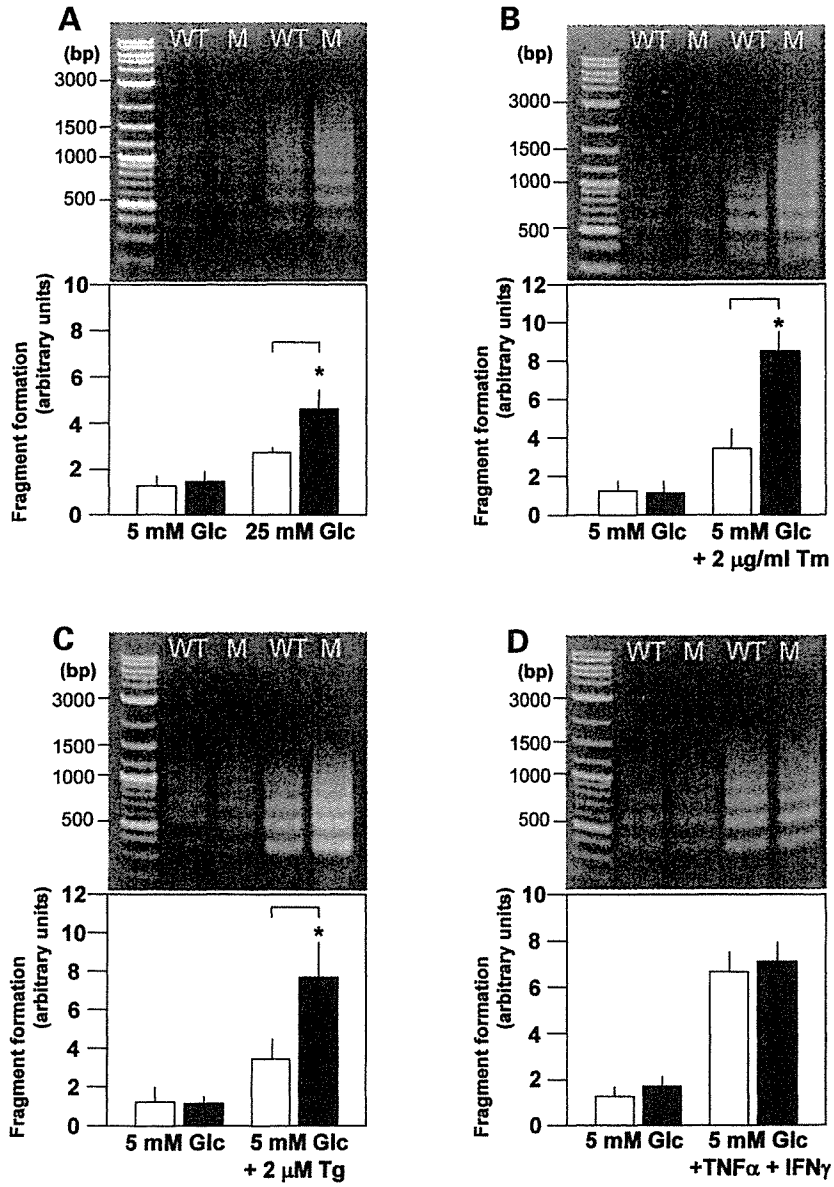

Figure 6. Increased apoptosis susceptibility in islets from mutant mice. (**A**) Islets from wild-type and mutant mice were cultured for 3 days in 5 and 25 mM glucose concentrations and DNA fragmentation was assessed by the LM-PCR method. (**B–D**) Islets from wild-type and mutant mice were treated with tunicamycin (Tm; 2 μg/ml) (B), thapsigargin (Tg; 2 μM) (C) for 24 h or with the combination of tumor necrosis factor-α (TNFα; 500 units/ml) and interferon-γ (IFNγ; 100 units/ml) (D) for 48 h and DNA fragmentation was assessed by the LM-PCR method; $n = 4–6$ experiments. $^*P < 0.05$.

contribution of genetic background is apparently complex. In any case, progressive β-cell loss was observed in mutant mice in both [(129Sv × B6) × B6]F2 and B6 strains, independent of the mouse genetic background. It is not surprising that mutant mice on the B6 background did not develop overt diabetes. Overt diabetes was known to be induced when >90% of the pancreas was removed (23), while the insulin content of mutant mouse pancreas at 36 weeks was decreased by 73% on the B6 background in this study.

The present data provide an intriguing clue that may help to elucidate WFS1 protein function. WFS1-deficient islets exhibited impaired insulin secretion in response to glucose and carbachol, which was restored by re-expression of WFS1 protein. In addition, overexpression of WFS1 protein in wild-type islets resulted in an increase in glucose- and carbachol-induced insulin secretion. These data from islets with different WFS1 protein levels demonstrated this protein to be involved directly in the regulation of insulin secretion. Furthermore, impaired calcium responses to glucose suggested that WFS1 protein is involved in regulation of calcium homeostasis in the β-cell. This notion is supported by the recent report that expression of WFS1 protein in *Xenopus* oocytes confers a novel cation channel activity (24). The present data also provide insight into the mechanism of β-cell loss in mice with a mutant *wfs1* gene. Although we rarely detected apoptotic cells in pancreatic sections from mutant mice, apoptosis cannot be excluded as a possible mechanism of β-cell loss, since our failure could presumably be due to slow progression of apoptosis *in vivo*

and rapid clearance of cells undergoing apoptosis, as was suggested recently in another animal model of diabetes (25). Increased apoptosis susceptibility in response to high glucose and ER-stress inducers, demonstrated in isolated islets from mutant mice, is likely to contribute to β-cell loss. In contrast, the apoptosis induced by exposure to tumor necrosis factor-α and interferon-γ, in which the ER-stress response is not involved, did not differ between wild-type and WFS1-deficient islets. Although the mechanism whereby high concentrations of glucose induce apoptosis is not completely understood at present (26,27), increased insulin translation in *perk*$^{-/-}$ islets indicates the ER-stress response or the unfolded protein response to be operative in islets cultured with high concentrations of glucose (28). Therefore, it is possible that increased DNA fragmentation in WFS1-deficient islets at 25 mM glucose could also be attributable to increased susceptibility to ER-stress-induced apoptosis. However, it remains to be clarified how WFS1 deficiency renders β-cells more susceptible to apoptosis, especially to ER-stress-induced apoptosis.

Recent studies showing β-cell mass to be decreased in human type 2 diabetes, due to increased β-cell apoptosis (29), have attracted considerable attention to this potential pathogenic mechanism of type 2 diabetes development. Therefore, maintaining β-cell mass is an important strategy for preventing diabetes as well as halting disease progression. Since the WFS1 protein is likely to belong to a novel family, elucidating the WFS1 protein function could lead to establishment of new treatments not only for Wolfram syndrome but also for more common forms of diabetes mellitus.

MATERIALS AND METHODS

Targeted disruption of the *wfs1* gene

The *wfs1* gene was cloned from a 129Sv mouse genomic DNA library using its cDNA probe (3). A targeting vector was constructed by inserting a neomycin-resistance gene at the *Sma*I site in exon 2 of the *wfs1* gene. The diphtheria toxin A chain expressing unit was inserted downstream (Fig. 2A). The *wfs1* gene targeting vector was microinjected into 129Sv embryonic stem cells. Homologous recombination was successful in two independent embryonic stem cell lines (lines 133 and 190). Positive chimeric male mice were then crossed with female C57BL/6J (B6) mice to produce *wfs1* heterozygous mice. Initial analyses demonstrated essentially the same phenotypes between the two lines, and therefore we have analyzed line 133 mice. In order to analyze animals with as homogenous a genetic background as possible, male *wfs1* heterozygous mice were backcrossed with female B6 mice for five successive generations. We also analyzed *wfs1* homozygous mice on the [(129Sv × B6) × B6]F2 hybrid background. The mice were kept in standard, specific pathogen-free conditions under a constant dark/light cycle. All animal experiments were approved by the local ethical committee for animal research at the Tohoku University.

Physiological studies

Control animals were age-matched siblings. Blood glucose levels in the non-fasting state were measured at 9:00–10:00 a.m. using a GluTest blood glucose monitor (Sanwa Chemicals, Tokyo, Japan). Serum insulin levels were determined by radioimmunoassay using a rat insulin RIA kit (Linco Research, St Charles, MO, USA). For oral glucose tolerance tests, animals after a 6 h fast were administered with 20% glucose solution (2 mg/g body weight) by gastric tubes. Whole-blood samples were collected from the tail tip at the indicated time points. Insulin tolerance tests were performed after a 6 h fast by an intraperitonial injection of human regular insulin (0.75 units/kg body weight).

Immunohistochemistry and morphometry

For brain sections, animals were anesthetized by ethylethel, and 4% formalin was perfused from the left ventricle. For pancreatic sections, the animals were killed by cervical dislocation. Dissected pancreas pieces were fixed in 4% formalin. Formalin-fixed paraffin-embedded sections of pancreas were de-paraffinized and re-hydrated. For insulin and glucagon staining, the sections were then incubated with a guinea pig anti-insulin IgG (DAKO Japan, Kyoto, Japan) diluted 1 : 1000 and a mouse anti-glucagon IgG (Sigma-Aldrich Japan, Tokyo, Japan) diluted 1 : 2000 for 1 h at room temperature. The anti-insulin and -glucagon primary antibodies were followed by a 45 min incubation with a fluorescein isothiocyanate (FITC)-conjugated anti-guinea pig IgG and a Texas Red-conjugated anti-mouse IgG (Jackson ImmunoResearch, West Grove, PA, USA). The antibody raised against the 290 amino acid α-mWFS1-N was described previously (30). Pancreatic sections incubated with the anti-WFS1 antibody were then stained with an FITC-conjugated anti-rabbit IgG (Jackson ImmunoResearch). Immunohistochemical analyses were performed, sacrificing at least four different animals for each condition. For measurements of β-cell area, more than 10 pancreatic tissue sections per animal were randomly selected, stained with anti-insulin IgG and eosin. Pancreatic area and β-cell area were each estimated using the intensity thresholding function of the NIH Image software. Four animals were analyzed for each group.

Pancreatic insulin and glucagon content

Pancreases were suspended in cold acid ethanol and minced by scissors, and left at −20°C for 48 h, with sonication every 24 h. Insulin content in the acid ethanol supernatant was determined with a rat insulin RIA Kit (Linco Research). Glucagon content in the same extract was measured by a glucagon RIA kit (Linco Research).

Islet studies

Construction of a recombinant adenovirus expressing murine WFS1 protein. A recombinant adenovirus AdCAGmWFS1, bearing an *EcoR*I fragment of murine WFS1 cDNA, was constructed by the method described previously (31,32). AdCAGlacZ expressing β-galactosidase was used as a control adenovirus. Isolated islets were infected with the recombinant adenoviruses at 1.2×10^5 particles per islet in 1.0 ml medium for 60 min.

Isolation and static incubation of islets. Islets isolated from age-matched wild-type and mutant siblings at 14–17 weeks were isolated by retrograde injection of collagenase (Serva, Heidelberg, Germany) into the pancreatic duct according to standard procedures. For secretion studies, batches of 10 islets (triplicates for each condition) were kept in Krebs–Ringer-bicarbonate-HEPES buffer [KRBH; 140 mM NaCl, 3.6 mM KCl, 0.5 mM NaH_2PO_4, 0.5 mM $MgSO_4$, 1.5 mM $CaCl_2$, 2 mM $NaHCO_3$, 10 mM HEPES (pH 7.4)] containing 0.1% BSA and stimulators indicated. Islet insulin content was measured following extraction by acid ethanol. Insulin was detected by radioimmunoassay.

Single cell Ca^{2+} measurement. Islets isolated from mice at 12–16 weeks were dispersed, plated on glass-bottomed dishes and cultured for 3 days before measurement. β-Cells were identified by adenovirus-mediated expression of green fluorescent protein driven by the insulin promoter (33). We performed experiments without adenovirus-mediated expression of green fluorescent protein, identifying β-cells with immunostaining after perfusion, and observed similar results (data not shown). Cells were incubated with 1 μM Fura 2-AM (Dojindo, Kumamoto, Japan) for 30 min, perfused with KRBH and excited at 340 and 380 nm. A cooled CCD camera (Hamamatsu Photonics, Shizuoka, Japan) mounted on a microscope (Leica Microsystems, Heerbrugg, Switzerland) was used to capture fluorescence images. Ca^{2+} rises were compared by calculating areas between Ca^{2+} curves and baselines for the 300 s after the onset of Ca^{2+} rises.

LM-PCR amplification of DNA fragments. Groups of 50 islets isolated from mice at 15–17 weeks of age were cultured for 3 days in RPMI with different glucose concentrations. In another series of experiments, groups of 50 islets were treated with 2 μg/ml tunicamycin (Sigma-Aldrich Japan), 2 μM thapsigargin (Alamone Labs, Jerusalem, Israel) or a combination of interferon-γ (100 units/ml; PeproTech, London, UK) and tumor necrosis factor-α (500 units/ml; PeproTech). Genomic DNA was isolated from treated islets using the DNeasy kit (Qiagen-Japan, Tokyo, Japan). The PicoGreen® dsDNA quantitation kit (Molecular Probes, Eugene, OR, USA) was used to determine the DNA concentrations. 200 ng of the genomic DNA was ligated with an adaptor, which has been generated by annealing two synthetic oligonucleotides 5′-AGCACTCTCGAGCCTCT CACCGCA-3′ and 5′-TGCGGTGAGAGG-3′. A portion of ligation mixture (30%) was used for the PCR amplification with a primer 5′-AGCACTCTCGAGCCTCTCACCGCA-3′. The resulting PCR products were run on 1.2% agarose gels. Intensities of ladders between 500 and 1000 bp were analyzed using the Scion Image software. In order to compare data from separate gels, band intensity was normalized to the average laddering of the control islets at 5 mM glucose.

Statistical analyses

Data are presented as mean ± SE, unless otherwise noted. Differences between wild-type and mutant animals were assessed by Student's *t*-test.

ACKNOWLEDGEMENTS

We thank Professor H. Takeshima, Dr Y. Ohwada and Professor T. Itoh, Tohoku University, for their help in Ca^{2+} imaging and immunohistochemical analyses. We are also grateful to N. Nishino, T. Wadatsu and N. Miyazawa, Otsuka GEN Research Institute, for their help in generation of WFS1-deficient mice. Y. Takahashi is gratefully acknowledged for her excellent technical assistance. This study was supported by Grants in Aid for Scientific Research (13204062) to Y.O. from the Ministry of Education, Science, Sports and Culture of Japan.

REFERENCES

1. Wolfram, D.J. and Wagener, H.P. (1938) Diabetes mellitus and simple optic atrophy among siblings: report on four cases. *Mayo Clinic Proc.*, **13**, 715–718.
2. Swift, M. and Swift, R.G. (2001) Psychiatric disorders and mutations at the Wolfram syndrome locus. *Biol. Psychiatry*, **47**, 787–793.
3. Inoue, H., Tanizawa, Y., Wasson, J., Behn, P., Kalidas, K., Bernal-Mizrachi, E., Mueckler, M., Marshall, H., Donis-Keller, H., Crock, P. *et al.* (1998) A gene encoding a transmembrane protein is mutated in patients with diabetes mellitus and optic atrophy (Wolfram syndrome). *Nat. Genet.*, **20**, 143–148.
4. Strom, T.M., Hoetnagael, K., Hofmann, S., Gekeler, F., Scharfe, C., Rabl, W., Gerbitz, K.D. and Meitinger, T. (1998) Diabetes insipidus, diabetes mellitus, optic atrophy and deafness (DIDMOAD) caused by mutations in a novel gene (wilframin) coding for a predicted transmembrane protein. *Hum. Mol. Genet.*, **7**, 2021–2028.
5. Cryns, K., Sivakumaran, T.A., Van den Ouweland, J.M., Pennings, R.J., Cremers, C.W., Flothmann, K., Young, T.L., Smith, R.J., Lesperance, M.M. and Van Camp, G. (2003) Mutational spectrum of the *WFS1* gene in Wolfram syndrome, nonsyndromic hearing impairment, diabetes mellitus, and psychiatric disease. *Hum. Mut.*, **22**, 275–287.
6. Bespalova, I.N., Van Camp, G., Bom, S.J., Brown, D.J., Cryns, K., DeWan, A.T., Erson, A.E., Flothmann, K., Kunst, H.P., Kurnool, P. *et al.* (2001) Mutations in the Wolfram syndrome 1 gene (WFS1) are a common cause of low frequency sensorineural hearing loss. *Hum. Mol. Genet.*, **15**, 2501–2508.
7. Young, T.L., Ives, E., Lynch, E., Person, R., Snook, S., MacLaren, L., Cater, T., Griffin, A., Fernandez, B., Lee, M.K. *et al.* (2001) Non-syndromic progressive hearing loss DFNA38 is caused by heterozygous missense mutation in the Wolfram syndrome gene *WFS1*. *Hum. Mol. Genet.*, **15**, 2509–2514.
8. Ohta, T., Koizumi, A., Kayo, T., Shoji, Y., Watanabe, A, Monoh, K., Higashi, K., Ito, S., Ogawa, O., Wada, Y. *et al.* (1998) Evidence of an increased risk of hearing loss in heterozygous carriers in a Wolfram syndrome family. *Hum. Genet.*, **103**, 470–474.
9. Minton, J.A., Hattersley, A.T., Owen, K., McCarthy, M.I., Walker, M., Latif, F., Barrett, T. and Frayling, T.M. (2002) Association studies of genetic variation in the *WFS1* gene and type 2 diabetes in U.K. populations. *Diabetes*, **51**, 1287–1290.
10. Awata, T., Inoue, K., Kurihara, S., Ohkubo, T., Inoue, I., Abe, T., Takino, H., Kanazawa, Y. and Katayama, S. (2000) Missense variations of the gene responsible for Wolfram syndrome (WFS1/wolframin) in Japanese: possible contribution of the Arg456His mutation to type 1 diabetes as a nonautoimmune genetic basis. *Biochem. Biophys. Res. Commun.*, **268**, 612–616.
11. Sequeira, A. Kim, C., Seguin, M., Lesage, A., Chawky, N., Desautels, A., Tousignant, M., Vanier, C., Lipp, O., Benkelfat, C. *et al.* (2003) Wolfram syndrome and suicide: evidence for a role of WFS1 in suicidal and impulsive behavior. *Am. J. Mol. Genet.*, **119B**, 108–113.
12. Takeda, K., Inoue, H., Tanizawa, Y., Matsuzaki, Y., Oba, J., Watanabe, Y., Shinoda, K. and Oka, Y. (2001) WFS1 (Wolfram syndrome 1) gene product: predominant subcellular localization to endoplasmic reticulum in cultured cells and neuronal expression in rat brain. *Hum. Mol. Genet.*, **10**, 477–484.
13. Hofmann, S., Philbrook, C., Gerbitz, K.D. and Bauer, M.F. (2003) Wolfram syndrome: structural and functional analyses of mutant and wild-type wolframin, the WFS1 gene product. *Hum. Mol. Genet.*, **12**, 2003–2012.

14. Kaufmann, R. (2002) Orchestrating the unfolded protein response in health and disease. *J. Clin. Invest.*, **110**, 1389–1398.
15. Harding, H.P. and Ron, D. (2002) Endoplasmic reticulum stress and the development of diabetes. *Diabetes*, **51** (Suppl. 3), S455–S461.
16. Rando, T.A., Horton, J.C. and Layzer, R.B. (1992) Wolfram syndrome: evidence of a diffuse neurodegenerative disease by magnetic resonance imaging. *Neurology*, **42**, 1220–1224.
17. Karasik, A., O'Hara, C., Srikanta, S., Swift, M., Soeldner, J.S., Kahn, C.R. and Herskowitz, R.D. (1989) Genetically programmed selective islet beta-cell loss in diabetic subjects with Wolfram's syndrome. *Diabetes Care*, **12**, 135–138.
18. Ferri, K.F. and Koemer, G. (2001) Organelle-specific initiation of cell death pathways. *Nat. Cell Biol.*, **3**, E255–E263.
19. Coleman, D.L. (1982) Diabetes–obesity syndromes in mice. *Diabetes*, **31** (Suppl. 2), 1–6.
20. Terauchi, Y., Matsui, J., Suzuki, R., Kubota, N., Komeda, K., Aizawa, S., Eto, K., Kimura, S., Nagai, R., Tobe, K. *et al.* (2003) Impact of genetic background and ablation of insulin receptor substrate (IRS)-3 on IRS-2 knock-out mice. *J. Biol. Chem.*, **278**, 14284–14290.
21. Ishihara, H., Tashiro, F., Ikuta, K., Asano, T., Katagiri, H., Inukai, K., Kikuchi, M., Yazaki, Y., Oka, Y. and Miyazaki, J. (1995) Inhibition of pancreatic beta-cell glucokinase by antisense RNA expression in transgenic mice: mouse strain-dependent alteration of glucose tolerance. *FEBS Lett.*, **371**, 329–332.
22. Kulkarni, R.N., Almind, K., Goren, H.J., Winnay, J.N., Ueki, K., Okada, T. and Kahn, C.R. (2003) Impact of genetic background on development of hyperinsulinemia and diabetes in insulin receptor/insulin receptor substrate-1 double heterozygous mice. *Diabetes*, **52**, 1528–1534.
23. Wier, G.C., Bonner-Wier, S. and Leahy, J.L. (1990) Islet mass and function in diabetes and transplantation. *Diabetes*, **39**, 401–405.
24. Osman, A.A., Saito, M., Makepeace, C, Permutt, M.A., Schlesinger, P. and Mueckler, M. (2003) Wolframin expression induces novel ion channel activity in endoplasmic reticulum membranes and increases intracellular calcium. *J. Biol. Chem.*, **278**, 52755–52762.
25. Reddy, S. Bradley, J., Ginn, S., Pathipati, P. and Ross, J.M. (2003) Immunohistochemical study of caspase-3-expressing cells within the pancreas of non-obese diabetic mice during cyclophosphamide-accelerated diabetes. *Histochem. Cell Biol.*, **119**, 451–461.
26. Donath, M.Y., Gross, D.J., Cerasi, E. and Kaiser, N. (1999) Hyperglycemia-induced beta-cell apoptosis in pancreatic islets of *Psammomys obesus* during development of diabetes. *Diabetes*, **48**, 738–744.
27. Maedler, K., Sergeev, P., Ris, F., Oberholzer, J., Joller-Jemelka, H.I., Spinas, G.A., Kaiser, N., Halban, P.A. and Donath, M.Y. (2002) Glucose-induced beta cell production of IL-1beta contributes to glucotoxicity in human pancreatic islets. *J. Clin. Invest.*, **110**, 851–860.
28. Harding, H.P., Zeng, H., Xhang, Y., Jungries, R., Chung, P., Plesken, H., Sabatini, D.D. and Ron, D. (2001) Diabetes mellitus and exocrine pancreatic dysfunction in *Perk*$^{-/-}$ mice reveals a role for translational control in secretory cell survival. *Mol. Cell*, 7, 1153–1163.
29. Butler, A.E., Janson, J., Bonner-Weir, S., Ritzel, R., Rizza, R.A. and Butler, P.C. (2003) β-Cell deficit and increased β-cell apoptosis in humans with type 2 diabetes. *Diabetes*, **52**, 102–110.
30. Cryns, K., Thys, S., van Laer, L., Oka, Y., Pfister, M., van Nassauw, L., Smith, R.J.H., Timmermans, J.P. and Van Camp, G. (2003) The *WFS1* gene, responsible for low frequent sensorineural hearing loss and Wolfram syndrome, is expressed in a variety of inner ear cells. *Histochem. Cell Biol.*, **119**, 247–256.
31. Miyake, S., Makimura, M., Kanegae, Y., Harada, S., Sato, Y., Takamori, K., Tokuda, C. and Saito, I. (1996) Efficient generation of recombinant adenoviruses using adenovirus DNA–terminal protein complex and a cosmid bearing the full-length virus genome. *Proc. Natl Acad. Sci. USA*, **93**, 1320–1324.
32. Niwa, H., Yamamura, K. and Miyazaki, J. (1991) Efficient selection for high-expression transfectants with a novel eukaryotic vector. *Gene*, **108**, 193–199.
33. Ishihara, H., Maechler, P., Gjinovci, A., Herrera, P.-L. and Wollheim, C.B. (2003) Islet β-cell secretion determines glucagon secretion from the neighboring α-cells. *Nat. Cell Biol.*, **5**, 330–335.

Available online at www.sciencedirect.com
SCIENCE DIRECT
ELSEVIER
Peptides 25 (2004) 1803–1808
PEPTIDES
www.elsevier.com/locate/peptides

Genetic variations at urotensin II and urotensin II receptor genes and risk of type 2 diabetes mellitus in Japanese

Susumu Suzuki[a,*], Zong Wenyi[a], Masashi Hirai[a], Yoshinori Hinokio[a], Chitose Suzuki[a], Takahiro Yamada[a], Shinsuke Yoshizumi[a], Michiko Suzuki[b], Yukio Tanizawa[c], Akira Matsutani[c], Yoshitomo Oka[a]

[a] *Division of Molecular Metabolism and Diabetes, Department of Internal Medicine, Tohoku University Graduate School of Medicine, Sendai 980-8574, Japan*
[b] *Faculty of Comprehensive Human Science, Shokei Gakuin College, Natori 981-1295, Japan*
[c] *Division of Molecular Analysis of Human Disorders, Department of Bio-Signal Analysis, Yamaguchi University Graduate School of Medicine, Ube, Japan*

Received 1 March 2004; accepted 24 March 2004
Available online 15 September 2004

Abstract

Urotensin II is among the most potent vasoactive hormones known and the urotensin II (UTS2) gene is localized to 1p36-p32, one of the regions reported to show possible linkage with type 2 diabetes in Japanese. When we surveyed genetic polymorphisms in the UTS2 and urotensin II receptor (GPR14) gene, we identified two SNPs with amino acid substitutions (designated T21M and S89N and an SNP in the promotor region (−605G>A) of the UTS2 gene, and two SNPs in the non-coding region of the GPR14 gene. We then studied these three SNPs in the UTS2 gene and two SNPs in the GPR14 gene in 152 Japanese subjects with type 2 diabetes mellitus and two control Japanese populations. The allele frequency of 89N was significantly higher in type 2 diabetic patients than in both elderly normal subjects ($P = 0.0018$) and subjects with normal glucose tolerance ($P = 0.0011$), whereas the allele frequency of T21M and −605G>A in the UTS2 gene and those of two SNPs in the GPR14 gene were essentially identical in these three groups. Furthermore, in the subjects with normal glucose tolerance, 89N was associated with significantly higher insulin levels on oral glucose tolerance test, suggesting reduced insulin sensitivity in subjects with 89N. These results strongly suggest that subjects with S89N in the UTS2 gene are more insulin-resistant and thus more susceptible to type 2 diabetes mellitus development.

Keywords: Urotensin II; Urotensin II receptor (GPR14); Single nucleotide polymorphism; Insulin resistance; Type 2 diabetes; Normal glucose tolerance

1. Introduction

Urotensin II is known to be most potent mammalian vasoconstrictor identified to date [1,4,7], exerting its biological effects via interaction with a member of a G-protein-coupled receptor superfamily, originally termed GPR14 [10,15,17].

The urotensin II (UTS2) gene is localized to 1p36-p32, one of the regions showing potential linkage with type 2 diabetes in Japanese affected sib-pairs [16]. The urotensin II receptor is a G-protein-coupled 7-transmembrane receptor, encoded in the GPR14 (G-protein-coupled receptor 14) gene located in 17q25.3 [10,15,17].

Type 2 diabetes is characterized by insulin resistance in insulin target tissues and impaired insulin secretion from pancreatic β-cells [6], both of which are caused by multiple genetic and environmental factors.

Recent evidence suggests that vascular factor dysfunction contributes to insulin resistance [2]. Plasma concentrations of

Abbreviations: SNP, single nucleotide polymorphism; OGTT, oral glucose tolerance test; NGT, normal glucose tolerance

* Corresponding author. Tel.: +81 22 717 7171; fax: +81 22 717 7177.
E-mail address: ssuzuki@int3.med.tohoku.ac.jp (S. Suzuki).

0196-9781/$ – see front matter © 2004 Elsevier Inc. All rights reserved.
doi:10.1016/j.peptides.2004.03.030

urotensin II was reported to be elevated in type 2 diabetic patients [20]. Urotensin II reportedly reduces glucose-induced insulin secretion in the perfused rat pancreas [19]. Urotensin II and its receptor may, therefore, contribute to the insulin-secretory defects and/or insulin resistance in type 2 diabetes.

We investigated genetic polymorphisms in the UTS2 [21] and GPR14 genes. We demonstrated a significant association between one SNP in the UTS2 gene and the prevalence of type 2 diabetes in Japanese. Further analysis suggested this SNP to be associated with insulin resistance. The possible contribution of the UTS2 gene to the pathogenesis of type 2 diabetes is discussed herein.

2. Subjects and methods

2.1. Subjects

We employed two control Japanese populations, as described previously [21]. One consisted of 122 elderly subjects who met stringent criteria for normal: 60 or more years of age, no past history of diabetes, hemoglobin A1c (HbA1c) less than 5.6%, and no third degree or closer relatives with diabetes. Applying these criteria reduced the possibility of including subjects who would later develop diabetes. Another consisted of 268 subjects undergoing routine annual health examinations and showing normal glucose tolerance (NGT) by 75 g oral glucose tolerance test (OGTT) using the WHO criteria. One hundred and fifty-two unrelated patients with type 2 diabetes were randomly recruited from the outpatient clinic of Tohoku University Hospital. Type 2 diabetes was diagnosed using the WHO criteria. The study protocol and genetic analysis of human subjects were reviewed and approved by the Tohoku University Institutional Review Board. Appropriate informed consent was obtained from all subjects examined, including the elderly control subjects and the NGT subjects. The insulin sensitivity index, HOMA(R), in the NGT subjects was assessed using the HOMA model [14]. ISI composite [13], another insulin sensitivity index, was calculated from plasma glucose and insulin concentrations during OGTT. Clinical characteristics of the elderly control subjects, NGT subjects, and type 2 diabetic patients are described previously [21].

2.2. Genomic DNA amplification and SNP identification

DNA was isolated from peripheral blood cells using a QIAamp DNA Mini Kit (QIAGEN, Hilden, Germany). To amplify coding regions and intron–exon boundaries from genomic DNA, a primer set was developed using the genomic sequence for UTS2. PCR was performed and each PCR fragment was directly sequenced in both directions (ABI PRISM 7700, PE Applied Biosystems, Mississauga, Canada). To screen for variants in UTS2, we sequenced the genomic DNA from 30 unrelated subjects with type 2 diabetes and that from 30 elderly control subjects.

2.3. SNP genotyping by PCR-RFLP

PCR-RFLP was employed to examine three SNPs in the UTS2 gene [12]. The nucleotide transition from C to T in codon 61 of the UTS2 gene, which results in amino acid transition from Thr to Met at amino acid position 21, generates an Hsp92 II site. This SNP was designated T21M for this study. The nucleotide transition from G to A in codon 266 (amino acid transition from Ser to Asp at amino acid position 89) eliminates an AfaI site. This SNP was designated S89N. SNP determination using PCR-RFLP was described previously [21].

2.4. SNP genotyping by hybridization probe assay on LightCycler

We used a hybridization probe assay on LightCycler to detect two SNPs in the GPR14 gene. Two fluorescent-labeled hybridization probes were designed for the simultaneous detection of the SNPs and detection of the variant alleles was performed by the melting curve analysis [11]. Two SNPs were detected with a single thermocycle protocol within 40 min. This method is rapid, highly sensitive, and high-throughput, and is thus suitable for routine clinical use and large-scale studies. The hybridization probes were designed according to guidelines recommended by Roche Diagnostics, Inc. The mutation probe was designed so that the investigated mutation is under the probe. The anchor probe was designed to probe within the 1–5 nucleotides. The melting temperature (T_m) of the mutation probe was designed to be approximately 5 °C lower than that of the anchor probe. The 5′-end of the probe placed downstream of the other probe was labeled with LC Red 640 and the 3′-end was phosphorylated. The 3′-end of the other probe was labeled by FITC. The primers and hybridization probes were synthesized by Nihon Gene Research Laboratories, Inc. (Sendai, Japan). All PCR condition used 4 mM $MgCl_2$, 0.5 μM of the two PCR primers each, 0.4 μM LC Red 640 labeled hybridization probes, 2 μl of LightCycler DNA Master Hybridization Mix (Roche, Mannheim, Germany) and 5–30 ng DNA in a final volume of 20 μl. The fluorometer gain setting was 20 in channel 2. The cycling program consisted of 15 s of initial denaturation at 95 °C and 40 cycles at 95 °C for 0 s (ramp rate 20 °C/s), 60 °C for 15 s (ramp rate 3.0 °C/s), and 72 °C for 9 s (ramp rate 20 °C/s). The analytical melting program was 95 °C for 20 s and 40 °C for 120 s, increasing to 85 °C at a ramp rate of 0.1 °C/s, with continuous fluorescence acquisition.

2.5. Statistical analysis

The association of SNP genotypes with diabetes was assessed by an analysis of contingency tables. Fisher's exact test was used to compare differences in proportions between groups. Pair-wise *t*-tests were used to compare differences in the least-squares means of quantitative traits between groups. Statistical analyses were performed using the statistical anal-

ysis package of SPSS (Statistical Package for the Social Sciences).

3. Results

3.1. UTS2

We identified two major SNPs with amino acid substitutions (designated T21M and S89N) and one major SNP in the promotor region (−605G>A) in the UTS2 gene, in Japanese control subjects and type 2 diabetic patients. Fig. 1 demonstrates the genetic structure and all genetic polymorphisms detected in the UTS2 gene in Japanese. The allelic frequency of other SNPs except these three SNPs was not so frequent.

A case–control study was performed by comparing the allele frequencies of UTS2 gene SNPs in 122 elderly control subjects, 268 NGT subjects, and 152 unrelated subjects with type 2 diabetes. The genetic frequency of SNP for Asn at amino acid 89 of prourotensin II was significantly higher in type 2 diabetic patients than in the elderly control subjects ($P = 0.0042$), as shown in Table 1 [21]. These elderly controls are expected to be "supernormal" in terms of having diabetogenic genes, since they met very stringent criteria: 60 or more years of age, no past history of diabetes, HbA1c less than 5.6%, and no third degree or closer relatives with diabetes. A highly significant difference in the genotype frequency of SNP-S89N was noted when type 2 diabetic patients were compared to the other controls, the NGT subjects ($P = 0.0005$). These findings were confirmed when allele frequencies were compared. The allele frequency of 89N was significantly higher in type 2 diabetic patients than in the elderly controls ($P = 0.0018$) and NGT ($P = 0.0011$) subjects. In contrast to the SNP-S89N findings, no difference in T21M-SNP was observed; the allele frequency of 21M was essentially identical in type 2 diabetic patients (36%), the elderly controls (34%) and NGT subjects (35%) (data not shown). There was no difference in the allelic or genotypic distribution of −605G>A between type 2 diabetic patients and the elderly control subjects (data not shown). There was no deviation of observed genotype frequencies from the Hardy-Weinberg expectation.

Table 1
Genotype and allele frequency of S89N in elderly controls, normal glucose tolerance (NGT) subjects, and type 2 diabetic patients

	Elderly controls	NGT	Type 2 diabetes
SNP-89 genotype			
Asn/Asn	3 (2.4%)	16 (6.0%)	11 (7.2%)
Ser/Asn	38 (31.2%)	74 (27.6%)	69 (45.4%)
Ser/Ser	81 (66.4%)	178 (66.4%)	72 (47.4%)
Sum	122	268	152
P-value	0.0042	0.0005	
SNP-89 allele			
Asn	44 (18.0%)	106 (19.8%)	91 (29.9%)
Ser	200 (82.0%)	430 (80.2%)	213 (70.1%)
Sum	244	536	304
χ_c^2	9.70	10.6	
P_c-value	0.0018	0.0011	
Odds ratio	1.94	1.73	

Means ± S.D. (vs. type 2 diabetes). Reproduced from [21] with permission from Springer-Verlag, Heidelberg.

The NGT subjects undergoing routine annual health examinations at Shimonoseki Kosei Hospital had their plasma insulin levels measured before and during OGTT. We therefore further studied the possible association of S89N with insulin sensitivity and/or insulin-secretory capacity in these NGT subjects ($n = 101$). The NGT subjects with the 89N allele had significantly elevated plasma insulin concentrations at 0 and 120 min and higher plasma glucose levels at 120 min of OGTT (Table 2). Their ∑PG, ∑PI (summations of plasma glucose and insulin levels during OGTT, respectively) and HbA1c values were also significantly greater than those of subjects with the 89S allele. It is noteworthy that the differences are small, as expected in NGT subjects, but statistically significant. Thus, even in NGT subjects, subjects with the 89N allele have minimally elevated plasma glucose, accompanied by slightly elevated plasma insulin, suggesting that the 89N allele contributes to insulin resistance. Indeed, HOMA(R) of NGT subjects with the 89N allele was significantly higher than that of subjects with the 89S allele ($P =$

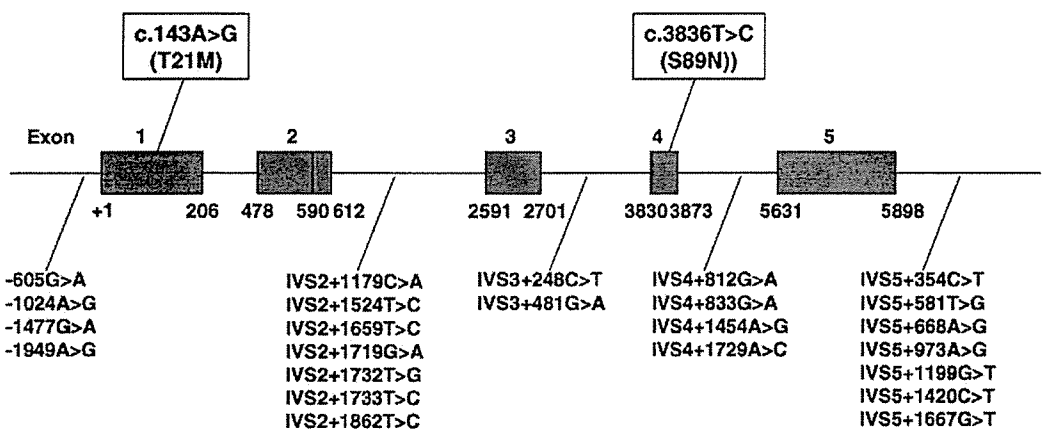

Fig. 1. Genetic polymorphisms in the urotensin II (UTS2) gene in Japanese. IVS: intervening sequence.

Table 2
Metabolic parameters in normal glucose tolerance (NGT) subjects classified according to S89N genotypes or alleles

Codon 89	*N*	IRI 0	IRI 120	∑BS	∑IRI	HOMA(R)	ISI composite
Asn/Asn	10	8.56 ± 2.24	43.9 ± 20.9	664 ± 104	212 ± 107	2.04 ± 0.58	3.09 ± 0.67
Ser/Asn	31	7.32 ± 2.30	35.5 ± 20.9	629 ± 95	167 ± 74	1.78 ± 0.58	3.48 ± 0.82
Ser/Ser	60	6.74 ± 1.70	28.1 ± 15.1	595 ± 79	150 ± 64	1.62 ± 0.46	3.75 ± 0.70
P (Asn/Asn vs. Ser/Ser)	0.0039	0.0051	0.017	0.014	0.0122	0.0071	
Asn	51	7.81 ± 2.31	38.8 ± 20.9	643 ± 98	185 ± 89	1.88 ± 0.58	3.33 ± 0.77
Ser	151	6.86 ± 1.74	29.6 ± 16.6	602 ± 83	154 ± 66	1.65 ± 0.49	3.70 ± 0.73
P (Asn vs. Ser)	0.0032	0.0016	0.0041	0.0089	0.0063	0.0023	

Means ± S.D. Adapted from [21] with permission from Springer-Verlag, Heidelberg.

0.0063). NGT subjects with the 89N allele had significantly lower ISI composite values than NGT subjects with the 89S allele ($P = 0.0023$). These data indicate that the 89N allele is associated with an insulin-resistant phenotype in NGT subjects. In contrast to SNP-S89N, the values described above are essentially identical in subjects with the 21T allele and those with the 21M allele (data not shown). There were also no association between the NGT subjects with −605G and the subjects with −605A (data not shown).

3.2. GPR14

The GPR14 gene is composed of a single large exon expanding to 1.17 kb, as shown in Fig. 2. We could not identify any SNP in the coding region of the GPR14 gene. We only found two major SNPs in the non-coding regions of GPR14 gene, designated −7836A/G and −7814C/T, in Japanese elderly control subjects and type 2 diabetic patients. A case–control study was performed by comparing the allele frequencies of the SNPs in 147 elderly control subjects and 155 unrelated subjects with type 2 diabetes. There were no difference in the genotypes or alleles of −7836A/G or −7814C/T; the allele frequency of −7836A/G or −7814C/T was essentially identical in type 2 diabetic patients and the elderly controls (Table 3). There was no deviation of observed genotype frequencies from the Hardy-Weinberg expectation.

The clinical parameter values are essentially identical in subjects with the −7836A allele and with the −7836G alleles. The values described above are essentially identical in subjects with or without −7814C/T (not shown).

Table 3
Genotype and allele frequencies of SNPs of the GPR14 gene in supernormal, and type 2 diabetic patients

	Elderly controls	DM
−7836A/G		
G/G	59 (49.6%)	58 (45.7%)
G/A	54 (45.4%)	57 (44.9%)
A/A	6 (5.0%)	12 (9.4%)
Sum	119	127
P-value	NS	
G	172 (72.3%)	173 (68.1%)
A	66 (27.7%)	81 (31.9%)
Sum	238	254
χ_c^2	0.825	
P_c-value	NS	
Odds ratio	1.22	
−7814C/T		
T/T	13 (8.8%)	16 (10.3%)
T/C	60 (40.8%)	65 (41.9%)
C/C	74 (50.3%)	74 (47.7%)
Sum	147	155
P-value	NS	
T	86 (29.3%)	97 (31.3%)
C	208 (70.7%)	213 (68.7%)
Sum	294	310
χ_c^2	0.208	
P_c-value	NS	
Odds ratio	0.91	

Means ± S.D. (vs. type 2 diabetes).

4. Discussion

This case–control association demonstrates a highly statistically significant difference in SNP-S89N frequency between the subjects with type 2 diabetes and the two control Japanese populations: *P*-values of allele frequency difference were 0.0018 versus the elderly controls and 0.0011 versus the NGT subjects [21]. Involvement of SNP-S89N in the development of diabetes was further supported by the results obtained in NGT subjects. Effects of SNP-S89N on glucose metabolism were evident even in NGT subjects. Plasma glucose appears to be slightly elevated in NGT subjects with the 89N allele as compared to those with the 89S allele, as demonstrated by higher glucose levels at 120 min of OGTT and higher HbA1c levels in NGT subjects with the 89N allele.

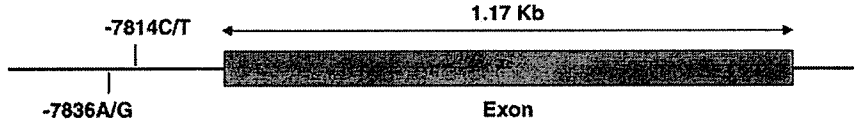

Fig. 2. Genetic polymorphisms in the urotensin II receptor (GPR14) gene in Japanese.

It is noteworthy that plasma insulin levels while fasting (time 0) and at 120 min of OGTT were also greater in those with the 89N allele than in those with the 89S allele. HOMA(R), which is calculated from fasting plasma glucose and insulin levels, is significantly greater in those with the 89N allele. These results strongly suggest that subjects with the 89N allele are more insulin-resistant than those with the 89S allele, and are thus more likely to develop diabetes.

The UTS2 gene is localized to 1p36, one of the regions showing potential linkage with type 2 diabetes in Japanese affected sib-pairs [16]. Linkage of this region with type 2 diabetes in Chinese and higher prevalence of the 89N allele in Chinese subjects with type 2 diabetes were recently reported in abstract form [9]. Our findings in the present case–control study are consistent with the report on Chinese subjects. Furthermore, the present study analyzing NGT subjects provides evidence that the 89N allele is associated with insulin resistance in Japanese. It would be of interest to determine whether SNP-S89N is associated with insulin resistance in other ethnic groups including Chinese.

Urotensin II is known to be most potent mammalian vasoconstrictor identified to date [1,4,7], exerting its biological effects via interaction with a member of a G-protein-coupled receptor superfamily, originally termed GPR14 [10,15,17]. Insulin induces endothelial-nitric-oxide-dependent vasodilatation. Recent data suggest that insulin's metabolic and vascular actions are closely linked [2]. Indeed, insulin-resistant states are associated with diminished insulin-mediated glucose uptake into peripheral tissues, and impaired insulin-mediated vasodilatation as well as impaired endothelium-dependent vasodilatation in response to the muscarinic receptor agonist acetylcholine. Several vasoactive hormones including endothelin-1 modulate insulin-mediated vasodilatation and induce insulin resistance in peripheral tissues and endothelium [2]. The present study is the first to show that SNP of the gene for the vasoactive hormone urotensin II contributes to insulin resistance.

Urotensin II may directly, rather than via vasoconstriction, affect glucose metabolism. Since appreciable numbers of urotensin II receptors are present in human skeletal muscle [12], urotensin II may regulate insulin sensitivity in skeletal muscle. The expression of urotensin II in the human liver also suggests a possible role of urotensin II in hepatic glucose homeostasis. In fish, urotensin II administration decreased hepatic glycogen content and increased glucose-6-phosphatase activity in the liver [18]. Further studies are needed to clarify the possible role of urotensin II in insulin signaling. Urotensin II receptor knockout mice are currently established and provide a direct evidence that the signaling of urotensin II occurred through its specific receptor, GPR14 [3]. Breeding GPR14 knockout mice onto a genetic background of diabetes (db/db, ob/ob mice, etc.) may be a good method for determining the influence of urotensin II and its receptor on the etiology of type 2 diabetes mellitus.

Urotensin II exerts a broad spectrum of biological actions in mammals: responses that influence cardiovascular, renal, pulmonary, central nervous system and endocrine function. Thus, urotensin II is proposed to contribute to human diseases including atherosclerosis, cardiac hypertrophy, pulmonary hypertension, hypertension and diabetes. It is a first report that the SNP in urotensin II gene contributes to the pathogenesis of type 2 diabetes. Future investigation should conduct to elucidate whether the SNPs in UTS2 and GPR14 genes associate with these polygenetic diseases, such as atherosclerosis, cardiac hypertrophy, pulmonary hypertension, hypertension.

Urotensin II is a cyclic dodecapeptide, derived from two splice variants of preproprotein with 124 or 138 amino acids through proteolytic cleavage by putative polybasic endopeptidase [1,5,8]. There are no previous reports indicating that the amino acid transition from Ser to Asn at position 89 influences the post-translational processing of preprourotensin II. Future investigation should focus on whether S89N affects the processing and/or secretion of urotensin II.

In conclusion, our results strongly suggest that subjects with S89N in the UTS2 gene are more insulin-resistant and thus more susceptible to type 2 diabetes mellitus development. The UTS2 gene is among the diabetogenic genes in the Japanese population.

Acknowledgements

We are grateful to all the patients who participated in this study and to their referring physicians. We would also like to thank the elderly controls and NGT subjects for participating. This study was supported by Grants in Aid for Creative Basic Research (10NP0210) and for Scientific Research (13204062) to Y.O. and Grants in Aid for Scientific Research (70216399) to S.S. from the Ministry of Education, Science, Sports and Culture of Japan and Grants to S.S. from Japan Diabetes Foundation and Japan Science and Technology Corporation (CREST).

References

[1] Ames RS, Sarau HM, Chambers JK, Willette RN, Aiyar NV, Romanic AM, et al. Human urotensin-II is a potent vasoconstrictor and agonist for the orphan receptor GPR14. Nature 1999;401:282–6.
[2] Baron AD. Insulin resistance and vascular function. J Diabetes Complications 2002;16:92–102.
[3] Behm DJ, Harrison SM, Ao Z, Maniscalco K, Pickering SJ, Grau EV, et al. Deletion of the UT receptor gene results in the selective loss of urotensin-II contractile activity in aortae isolated from UT receptor knockout mice. Br J Pharmacol 2003;139:464–72.
[4] Bohm F, Pernow J. Urotensin II evokes potent vasoconstriction in humans in vivo. Br J Pharmacol 2002;135:25–7.
[5] Coulouarn Y, Lihrmann I, Jegou S, Anouar Y, Tostivint H, Beauvillain JC, et al. Cloning of the cDNA encoding the urotensin II precursor in frog and human reveals intense expression of the urotensin II gene in motoneurons of the spinal cord. Proc Natl Acad Sci USA 1998;95:15803–8.
[6] DeFranzo RA, Bonadonna RC, Ferrannini E. Pathogenesis of NIDDM: a balanced overview. Diabetes Care 1992;15:318–68.
[7] Douglas SA, Ohlstein EH. Human urotensin-II, the most potent mammalian vasoconstrictor identified to date, as a therapeutic target

for the management of cardiovascular disease. Trends Cardiovasc Med 2000;10:229–37.
[8] Elshourbagy NA, Douglas SA, Shabon U, Harrison S, Duddy G, Sechler JL, et al. Molecular and pharmacological characterization of genes encoding urotensin-II peptides and their cognate G-protein-coupled receptors from the mouse and monkey. Br J Pharmacol 2002;136:9–22.
[9] Ji L, Zhu F, Luo B. The role of urotensin II gene in the genetic susceptibility to type 2 diabetes in Chinese population. Diabetes 2002;51(Suppl 2):260.
[10] Liu Q, Pong SS, Zeng Z, Zhang Q, Howard AD, Williams Jr DL, et al. Identification of urotensin II as the endogenous ligand for the orphan G-protein-coupled receptor GPR14. Biochem Biophys Res Commun 1999;266:174–8.
[11] Lyon E. Mutation detection using fluorescent hybridization probes and melting curve analysis. Expert Rev Mol Diagn 2001;1:92–101.
[12] Maguire JJ, Kuc RE, Davenport AP. Vasoconstrictor activity of novel endothelin peptide, ET-1(1-31), in human mammary and coronary arteries in vitro. Br J Pharmacol 2001;134:1360–6.
[13] Matthews DR, Hosker JP, Rudenski AS, Naylor BA, Treacher DF, Turner RC. Homeostasis model assessment: insulin resistance and beta-cell function from fasting plasma glucose and insulin concentrations in man. Diabetologia 1985;28:412–9.
[14] Matsuda M, DeFronzo RA. Insulin sensitivity indices obtained from oral glucose tolerance testing: comparison with the euglycemic insulin clamp. Diabetes Care 1999;22:1462–70.
[15] Mori M, Sugo T, Abe M, Shimomura Y, Kurihara M, Kitada C, et al. Urotensin II is the endogenous ligand of a G-protein-coupled orphan receptor SENR (GPR14). Biochem Biophys Res Commun 1999;265:123–9.
[16] Mori Y, Otabe S, Dina C, Yasuda K, Populaire C, Lecoeur C, et al. Genome-wide search for type 2 diabetes in Japanese affected sib-pairs confirms susceptibility genes on 3q, 15q, and 20q and identifies two new candidate loci on 7p and 11p. Diabetes 2002;51:1247–55.
[17] Nothacker HP, Wang Z, McNeill AM, Saito Y, Merten S, O'Dowd B, et al. Identification of the natural ligand of an orphan G-protein-coupled receptor involved in the regulation of vasoconstriction. Nat Cell Biol 1999;1:383–5.
[18] Sheridan MA, Plisetskaya EM, Bern HA, Gorbman A. Effects of somatostatin-25 and urotensin II on lipid and carbohydrate metabolism of coho salmon *Oncorhynchus kisutch*. Gen Comp Endocrinol 1987;66:405–14.
[19] Silvestre RA, Rodriguez-Gallardo J, Egido EM, Marco J. Inhibition of insulin release by urotensin II – a study on the perfused rat pancreas. Horm Metab Res 2001;33:379–81.
[20] Totsune K, Takahashi K, Arihara Z, Sone M, Ito S, Murakami O. Increased plasma urotensin II levels in patients with diabetes mellitus. Clin Sci (London) 2003;104:1–5.
[21] Wenyi Z, Suzuki S, Hirai M, Hinokio Y, Tanizawa Y, Matsutani A, et al. Role of urotensin II gene in genetic susceptibility to type 2 diabetes mellitus in Japanese subjects. Diabetologia 2003;46:972–6.

K. Takahashi
J. Satoh
Y. Kojima
K. Negoro
M. Hirai
Y. Hinokio
Y. Kinouchi
S. Suzuki
N. Matsuura
T. Shimosegawa
Y. Oka

Promoter polymorphism of *SLC11A1* (formerly *NRAMP1*) confers susceptibility to autoimmune type 1 diabetes mellitus in Japanese

Key words:
antigen-presenting cells; insulin-dependent diabetes mellitus; macrophage activation; macrophages; natural resistance; NRAMP; polymorphism; SLC11A1

Acknowledgments:
We thank Ms C. Suzuki for technical assistance. This study was supported by a grant-in-aid for Scientific Research on Priority Areas (C) 'Medical Genome Science' from the Ministry of Education, Culture, Sports, Science and Technology of Japan (to YO) and grants from the Japan Society for the Promotion of Science (14570401), the Takeda Medical Research Foundation, and the Japan Insulin Study Group Foundation (to KT).

Abstract: Defective function of antigen-presenting cells has been postulated to be one of the non-HLA-linked susceptibility factors for type 1 diabetes mellitus, though the underlying genetic factors remain unclear. SLC11A1 (formerly NRAMP1), a divalent cation transporter, plays a crucial role in macrophage activation. We performed a case-control study in 224 healthy and 95 type 1 diabetic Japanese subjects, examining the length polymorphisms in the promoter region (−377 to −222) of *SLC11A1*, which may influence transcriptional activity. Alleles designated 2, 3, and 7 have been identified in Japanese subjects. The frequency of allele 7 was significantly higher in subjects with type 1 diabetes (9.47%) than in the healthy controls (4.46%). The difference is more marked in the subpopulation of Japanese subjects with type 1 diabetes; diabetic subjects with at least one protective HLA class II allele and those without any susceptibility HLA class II haplotypes, DR4-DQ4 or DR9-DQ9, had a much higher allele 7 frequency than controls. These findings suggest that the novel promoter polymorphism of *SLC11A1* influences the susceptibility to type 1 diabetes in Japanese subjects.

Authors' affiliation:

K. Takahashi[1]
J. Satoh[1]
Y. Kojima[2]
K. Negoro[2]
M. Hirai[1]
Y. Hinokio[1]
Y. Kinouchi[2]
S. Suzuki[1]
N. Matsuura[3]
T. Shimosegawa[2]
Y. Oka[1]

[1]Division of Molecular Metabolism and Diabetes, Department of Internal Medicine, Tohoku University Graduate School of Medicine, Sendai, Japan

[2]Division of Gastroenterology, Department of Internal Medicine, Tohoku University Graduate School of Medicine, Sendai, Japan

[3]Department of Pediatrics, Kitasato University School of Medicine, Sagamihara, Japan

Correspondence to:
Dr Kazuma Takahashi, MD, PhD
Division of Molecular Metabolism and Diabetes
Tohoku University Graduate School of Medicine
1-1 Seiryo-machi, Aoba-ku
Sendai 980-8574, Japan
Tel.: +81-22-717-7171
Fax: +81-22-717-7177
e-mail: ktakahashi@int3.med.tohoku.ac.jp

Received 21 May 2003, revised 11 September 2003, accepted 30 September 2003

Tissue Antigens 2004: **63:** 231–236
Printed in Denmark.

Antigen-presenting cells (APCs) strongly influence several qualitative and quantitative aspects of T-cell activation (1–4). In humans at risk for type 1 diabetes mellitus and in the non-obese diabetic (NOD) mouse, the murine model for this disease, defects in APCs contribute to low levels of T-cell activation, poor interleukin-2 (IL-2) production, and deficient activation of regulatory T cells (5–8). Defective APC function may predispose to autoimmunity through reduction in signals required for activation-induced T-cell death or regulatory T-cell responses, both of which are important mechanisms for peripheral tolerance (3, 9, 10). Factors contributing to APC dysfunction in type 1 diabetes in humans and in NOD mouse include those encoded by the major histocompatibility complex (MHC) class II region and non-MHC alleles. The unique H-2^{g7} molecule of the NOD mouse plays a central role, as the inability of NOD APCs to activate immunoregulatory T cells in a syngeneic mixed lymphocyte reaction was associated with the homozygous expression of H-2^{g7} (11), and

marrow-derived APCs from NOD congenic mice expressing the diabetes-resistant H-2^{nb1} haplotype of NOD mice inhibited the development of diabetogenic T cells from NON marrow (12). In addition to the MHC, multiple non-MHC-susceptibility genes contribute to the pathogenesis of insulin-dependent diabetes mellitus (IDDM) in the NOD mouse and in humans (13). The identities of these genes and their contributions to APC dysfunction however have not been defined.

SLC11A1 (formerly NRAMP1), a divalent cation transporter (14), plays important roles early in the macrophage activation and displays multiple pleiotropic effects on macrophage function, including the expression of chemokines, IL-1β, tumor necrosis factor α-inducible nitric oxide synthase, and MHC class II molecules (14). *SLC11A1* is located on human chromosome 2 (2q35), which includes at least three human type 1 diabetes-susceptible loci [*IDDM7* (15), *IDDM12* (16), and *IDDM13* (17)]. Several candidate genes in this region have already been focused on in several association studies carried out on various genetic backgrounds, and association of *CTLA-4* (18) in *IDDM12* and of *NeuroD/BETA2* (19) in *IDDM13* with type 1 diabetes has been suggested in Japanese. However, the multiple pleiotropic effect of SLC11A1 on macrophage function, as well as the report by Hill et al. (20) that proposed SLC11A1 as a prime candidate for a mouse type 1 diabetes locus, *Idd5.2*, the homolog of human *IDDM13*, prompted us to look for association of *SLC11A1* with human type 1 diabetes mellitus.

In the promoter region of *SLC11A1*, six different alleles of the polymorphism have been reported at functional Z-DNA forming repeats in Caucasian. Several studies support the hypothesis that this functional repeat polymorphism contributes to the susceptibility to autoimmune and infectious diseases. In rheumatoid arthritis and juvenile rheumatoid arthritis, family-based transmission disequilibrium testing or case-control analyses have all shown an allelic association with allele 3, possessing the strongest activity driving the SLC11A1 expression, while allele 2 with weaker promoter activity is significantly protective. Conversely, allele 2 displays positive association with infectious diseases including tuberculosis and leprosy and is protective in autoimmune diseases (14). So far, the association of allele 2 and allele 3 in *SLC11A1* polymorphism with type 1 diabetes mellitus is limited; allele 2 is negatively associated with a subpopulation of early-onset type 1 diabetes in Japanese, but not with whole population (21), and allele 3 was significantly transmitted to type 1 diabetic siblings in UK families that have a first- or second-degree relative with rheumatoid arthritis (22).

Recently, Kojima et al. identified the allele with 15 GT repeats in Japanese (23). This novel allele, named allele 7, is the same in length as, but different in sequences from, allele 1 reported in Caucasians. Contrary to the previous observations on autoimmune diseases, they could confirm neither positive association of allele 3 nor negative association of allele 2 with inflammatory bowel diseases, but found allele 7 susceptible. In the present study, we have extended their observation on Inflammatory Bowel Disease (IBD) to type 1 diabetes mellitus and performed a case-control study to explore the pathogenic role of the *SLC11A1*-promoter polymorphism in type 1 diabetes mellitus in Japanese.

Materials and methods

Subjects

After obtaining approval from the ethics committee of the Tohoku University Graduate School of Medicine and informed consent from all subjects, blood samples were collected from 224 healthy subjects (115 males and 109 females), and 95 type 1 diabetic subjects (43 males and 52 females). Mean age at onset (±SD) was 15.7 ± 11.1 years (range 1–36 years). All the subjects were Japanese. All type 1 diabetic subjects were ketosis prone, insulin dependent since diagnosis, and positive for either autoantibody to glutamic acid decarboxylase (GAD) or insulinoma-associated protein-2 (IA-2). The mean ages (±SD) of control and diabetic subjects were 29.5 ± 12.1 and 27.6 ± 11.8 years, respectively.

Autoantibodies

Anti-GAD autoantibody was assayed using an immunoassay kit, GAD Ab Cosmic (Cosmic, Tokyo, Japan) (24). Anti-tyrosine phosphatase IA-2 autoantibody was measured by precipitation of [^{35}S] methionine-labeled recombinant proteins synthesized after transcription translation in a TNT^{TM}-coupled reticulocyte lysate system (Promega, Madison, WI) (5).

Determination of length polymorphisms and identification of their corresponding sequences

Genomic DNAs were obtained from peripheral blood leucocytes by standard phenol–chloroform extraction and ethanol precipitation or by utilizing an NA-1000 Automated Nucleic Acid Extraction Machine (Kurabo, Osaka, Japan). To identify the polymorphism, the promoter region spanning −377 to −222 relative to the transcription start site was amplified by polymerase chain reaction (PCR) using a thermal cycler (Perkin-Elmer, Foster City, CA). The PCR primers were as follows: 5'hexachlorofluorescein (HEX)-labeled sense (HEX-NRAMP-S1), 5'-CATTAGGCCAACGAGGGGTCTT-3'; and non-labeled antisense (NRAMP-as1), 5'-TCCTGCCCCTTGCGTATTCATG-3'. PCR conditions were as follows: 45 cycles of denaturing at